

# Experimental Digital Simulation of Quantum Tunneling in a NMR Quantum Simulator

Guan Ru Feng<sup>1,2</sup>, Yao Lu<sup>1,2</sup> and Gui Lu Long<sup>1,2</sup>

<sup>1</sup>*State Key Laboratory of Low-dimensional Quantum Physics and Department of Physics, Tsinghua University, Beijing 100084, P. R. China*

<sup>2</sup>*Tsinghua National Laboratory for Information Science and Technology, Beijing 100084, P. R. China*

(Dated: October 31, 2018)

It is well-known that quantum computers are superior to classical computers in efficiently simulating quantum systems. Here we report the first experimental simulation of the quantum tunneling through potential barriers, a widespread phenomenon of unique quantum feature, via NMR techniques. Our experiment is based on the digital simulation algorithm that discretizes continuous space and time into lattices, and it uses only two spin-1/2 nuclei without the need of ancillary qubits. The occurrence of quantum tunneling through a barrier is clearly observed through the experimental result. This experiment has clearly demonstrated the viability of quantum simulation of a wide range of quantum phenomena with not only discrete, but also continuous degrees of freedom.

PACS numbers: 03.65.Xp, 03.67.Ac, 03.67.Lx, 07.57.Pt

Quantum computation has now become the subject of intense investigation ever since Feynman discussed the likelihood to simulate one quantum system by another [1]. Recent years have witnessed fruitful results in the development of quantum computation. Not only has Feynman's conjecture been generally confirmed, but also has it been demonstrated that quantum computers can solve problems with high efficiency which is beyond the capability of classical computers, such as Shor's quantum algorithm for integer factorization [2] and Grover's quantum search algorithm [3]. As conjectured by Feynman, simulation of the dynamics of quantum systems is one of the most important aims of quantum computation. Quantum simulations, such as simulation of many-body interaction Hamiltonian[4–6], dynamics of entanglement[7], quantum phase transition[8], calculations of molecular properties[9, 10], and so on, have been demonstrated in experiments. Quantum simulation is especially attractive in that via digital quantum particle simulations [11, 12] it provides an exponential improvement compared with classical computation, for example, making it a promising candidate in analysis of chemical reactions [13, 14].

As a unique fundamental concept in quantum mechanics, quantum tunneling plays an essential role in many quantum phenomena such as the tunneling of superconducting Cooper pairs [15], and its property is widely applied in modern experimental techniques such as the tunnel diode [16], the scanning tunneling microscope [17] and so on. Quantum tunneling is of continuous interest. Sornborger [18] proposed a small scale digital simulation algorithm for demonstrating the one particle wavefunction tunneling in a double well potential using a quantum information processor. In this paper, we realized the algorithm via room temperature liquid state NMR of two qubits. Using the digital simulation algorithm, the continuous process of one-dimensional tunneling of a particle through a potential barrier is clearly

demonstrated. Our experiment has shown definitely that with a very few qubits, interesting tunneling dynamics is simulated with a gate count that is within reach of current quantum architectures.

In the digital quantum simulation [11, 18], the one-dimensional wave function  $\psi(x, t)$  of a single particle moving in square-like potential with Schrödinger equation as

$$i \frac{\partial}{\partial t} \psi(x, t) = \left[ \frac{\hat{P}^2}{2m} + V(\hat{X}) \right] \psi(x, t), \quad (1)$$

where  $\hat{P}$  and  $\hat{X}$  are momentum and position operators, respectively. Throughout the text we set  $\hbar$  to be 1. In the Schrödinger picture the evolution of the wave function with time can be straightforwardly given as

$$|\psi(x, t + \Delta t)\rangle = e^{-i \left[ \frac{\hat{P}^2}{2m} + V(\hat{X}) \right] \Delta t} |\psi(x, t)\rangle, \quad (2)$$

which can be further decomposed according to the Trotter formula [11, 18],

$$|\psi(x, t + \Delta t)\rangle = \left[ e^{-i \frac{\hat{P}^2}{2m} \Delta t} e^{-i V(\hat{X}) \Delta t} + O(\Delta t^2) \right] |\psi(x, t)\rangle. \quad (3)$$

For sufficiently small time step  $\Delta t$ , Eq. (3) can be approximated as

$$|\psi(x, t + \Delta t)\rangle = e^{-i \frac{\hat{P}^2}{2m} \Delta t} e^{-i V(\hat{X}) \Delta t} |\psi(x, t)\rangle. \quad (4)$$

Similarly, the continuous degree of coordinate  $x$  is also discretized. Suppose  $\psi(x, t)$  is continuous on the region  $0 < x < L$ , with a periodic boundary condition  $\psi(x + L, t) = \psi(x, t)$ .  $x$  is discretized into a lattice with spacing  $\Delta l$  and the wave function is stored in an  $n$ -qubit quantum register

$$\psi(x, t) \rightarrow \sum_{k=0}^{2^n-1} \psi(x_k, t) |k\rangle, \quad (5)$$

where  $x_k = (k + \frac{1}{2})\Delta l$ ,  $\Delta l = \frac{L}{2^n}$ , and  $|k\rangle$  is the lattice basis state corresponding to the binary representation of the number  $k$ . Apparently, Eq. (5) gives a good approximation to the wave function in the limit  $n \rightarrow \infty$ .

As a small scale demonstration, we will investigate the 2-qubit simulation from now on. In this case, the four basis state  $|00\rangle$ ,  $|01\rangle$ ,  $|10\rangle$  and  $|11\rangle$  register four lattice points 1, 2, 3 and 4 as discretized position variable of the particle.

The next problem lies in the construction of the kinetic and the potential operators for the discretized wave function. As the potential operator  $V(\hat{X})$  is a function of the coordinate operator  $x$ , it is diagonal in the coordinate representation, though discretized now. In a  $n$ -qubit discretized grid,  $V$ , a diagonal matrix in the coordinate representation, can always be decomposed as

$$V = \sum_{i_1, i_2, \dots, i_n=3}^4 c_{i_1 i_2 \dots i_n} \otimes_{k=1}^n \sigma_{i_k}, \quad (6)$$

where each term in the summation corresponds to an diagonal entry with coefficient  $c_{i_1 i_2 \dots i_n}$ ,  $\sigma_3$  is the pauli matrix  $\sigma_z = \begin{pmatrix} 1 & 0 \\ 0 & -1 \end{pmatrix}$  and  $\sigma_4 = I$  is the identity matrix in two dimension. One simple example of a potential with the form of Eq. (6) is

$$V = V_0 I \otimes \sigma_z, \quad (7)$$

which corresponds to a double well potential of amplitude  $2V_0$ , with the two peak  $V_0$  at 00 and 10 and the values  $-V_0$  at the two bottoms at 01 and 11. This double-well potential can therefore be implemented using only a single qubit gate

$$P = e^{-iV(\hat{X})\Delta t} = I \otimes e^{-iV_0\sigma_z\Delta t}. \quad (8)$$

The kinetic energy operator can be found with the help of quantum Fourier transformation(QFT). The kinetic energy operator is diagonal in the momentum representation, thus by QFT, it can be expressed in the coordinate representation,

$$\frac{\hat{P}^2}{2m} = F^{-1} \frac{\pi^2}{4} \Pi F, \quad (9)$$

where we have taken  $m = 1/2$ ,  $\Pi = \text{diag}[0, 4, 1, 1]$  and

$$F = \frac{1}{2} \sum_{j,k=0}^3 e^{\frac{1}{2}i\pi jk} |j\rangle \langle k|. \quad (10)$$

is the discrete Fourier transformation operator. QFT can be readily implemented in quantum circuits via a series of Hadamard gate and controlled-phase gate [19]

$$F = H_2 R_{\frac{\pi}{2}} H_1, \quad (11)$$

where  $H_1$  and  $H_2$  are Hadamard gates on the first and the second qubit, respectively, and  $R_{\frac{\pi}{2}} = \text{diag}[1, 1, 1, i]$  is the

two-qubit controlled phase gate. The operator  $e^{-i\frac{\hat{P}^2}{2m}\Delta t}$  can be expressed in the two-qubit lattice can be written as

$$e^{-i\frac{\hat{P}^2}{2m}\Delta t} = F^{-1} \Phi_{\pi} Z_1 Z_2 F, \quad (12)$$

where

$$\Phi_{\pi} = \exp[-i\frac{3\pi^2}{4} R_{\pi} \Delta t], \quad (13)$$

$R_{\pi} = R_{\frac{\pi}{2}} R_{\frac{\pi}{2}}$  and

$$Z_1 = \exp[i\frac{\pi^2}{4} \sigma_z \otimes I \Delta t], \quad (14)$$

$$Z_2 = \exp[i\frac{3\pi^2}{4} I \otimes \sigma_z \Delta t]. \quad (15)$$

Thus the time-dependent Schrödinger Eq. (4) can be rewritten as

$$\sum_{k=0}^3 \psi(x_k, t + \Delta t) |k\rangle = F^{-1} \Phi_{\pi} Z_1 Z_2 F P \sum_{k=0}^3 \psi(x_k, t) |k\rangle. \quad (16)$$

We experimentally studied the time evolution of a particle moving in a double-well potential in a digital algorithm in a 2-qubit system via the room temperature NMR system. A d6-acetone solution of  $^{13}\text{C}$ -labeled chloroform at 295K is used where  $^1\text{H}$  (with a resonance frequency 400.130 MHz) encodes the first qubit and  $^{13}\text{C}$  (with a resonance frequency 100.613 MHz) encodes the second qubit.

From Eq. (16) the one time step evolution quantum circuit for our simulation is straightforwardly obtained, as drawn in Fig. 1. The corresponding pulse sequences for implementing the operations in the quantum circuit is exhibited in Fig. 2.

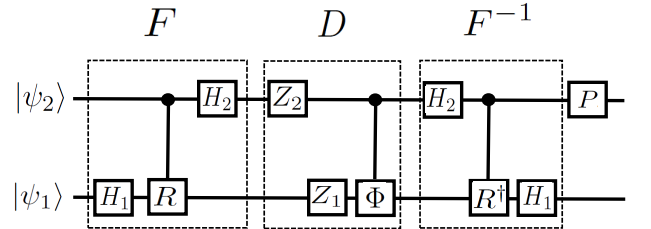


Figure 1: Quantum circuit for one time step simulation.  $|\psi_1\rangle$  and  $|\psi_2\rangle$  are the input states of the first and the second qubit, respectively.

In our experiments we set the time interval to be  $\Delta t = \frac{1}{10}$  and the amplitude of the potential  $2V_0 = 20$ . We simulated the situation in which the particle is initially trapped inside one of the two wells by preparing the pseudo-pure state  $|01\rangle$  from the thermal equilibrium [20] as the initial state with a high experimental realized fidelity  $f = 99.89\%$  (see Fig. 3) which is given by

$$f = \frac{\text{trace}(\rho_{ex}\rho_{th})}{\sqrt{\text{trace}(\rho_{ex}^2)\text{trace}(\rho_{th}^2)}} \quad (17)$$

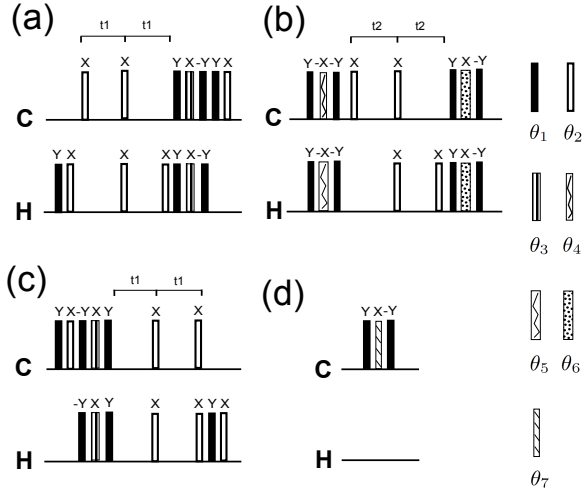


Figure 2: Pulse sequences to implement the circuit in Fig. 1, where (a), (b), (c), (d) realize the four operations  $F$ ,  $D$ ,  $F^{-1}$  and  $P$  respectively. The time periods  $t_1 = \frac{1}{8J} = 580.9\mu s$  and  $t_2 = \frac{\pi}{40J} = 365.0\mu s$  represent the free evolution durations under the  $J$  coupling (for chloroform  $J = 215.2Hz$ ). The bars represent single-qubit rotation pulses with the phases as shown and seven different fillings that are depicted to the right, indicating different rotation angles as  $\theta_1 = \frac{\pi}{2}$ ,  $\theta_2 = \pi$ ,  $\theta_3 = \frac{\pi}{4}$ ,  $\theta_4 = \frac{\pi^2}{40}$ ,  $\theta_5 = \frac{\pi^2}{10}$ ,  $\theta_6 = \frac{\pi^2}{20}$ ,  $\theta_7 = 2$ , respectively.

where  $\rho_{th}$  is the theoretical density matrix, and  $\rho_{ex}$  is the experimental density matrix.

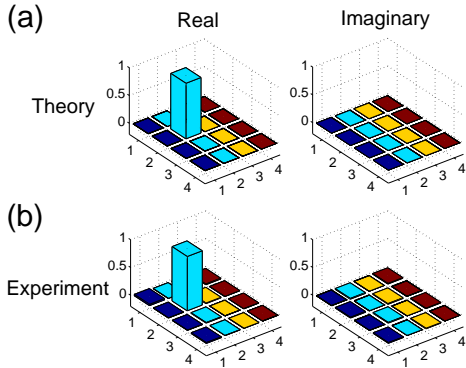


Figure 3: (Color online). The real and imaginary parts of (a) the density matrix elements of the  $|01\rangle$  state; (b) the density matrix elements reconstructed by QST for the the initial  $|01\rangle$  state in our experiment.

In order to observe the tunneling process of the particle, nine experiments have been carried out in which the pulse sequence in Fig. 2 has been performed 1  $\sim$  9 times, respectively. Quantum state tomography (QST) is performed on the density matrices of the final states after 1 to 8 steps([21, 22]). The diagonal elements which correspond to the simulation of the probability distribution of the particle are illustrated in Fig. 6 comparing

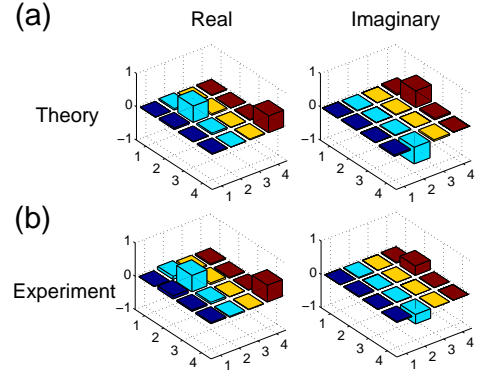


Figure 4: (Color online). The real and imaginary parts of (a) the theoretically calculated density matrix elements after nine steps of evolution with in a double well potential; (b) the experimental density matrix elements reconstructed by QST after the nine steps of evolution with in a double well potential.

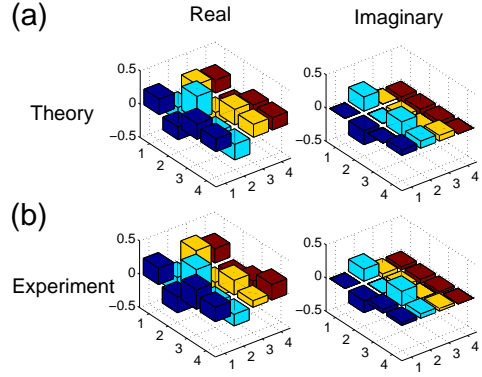


Figure 5: (Color online). The real and imaginary parts of (a) the theoretically calculated density matrix elements after nine steps of evolution without double well potential; (b) the experimental density matrix elements reconstructed by QST after nine steps of evolution without the double well potential.

with theoretical results. The full density matrix of the final state after 9 steps in our experiment is shown fully in Fig. 4 along with the theoretical results. The fidelity of the experimental density is determined by Eq. 17) to be 95.48%. As is depicted in Fig. 6 (b) the whole evolution process of a single particle's probability distribution in the double well potential can be obtained through our 9-step experiment. It can be clearly observed that the particle tunnels through the potential barrier between the two wells, while its probability to be found in the barrier is scarce, which accords well with the theoretical calculations in Fig. 6 (a).

For the sake of comparison we also studied the simulation of the evolution of a free particle with zero potential using basically the same experimental schemes and

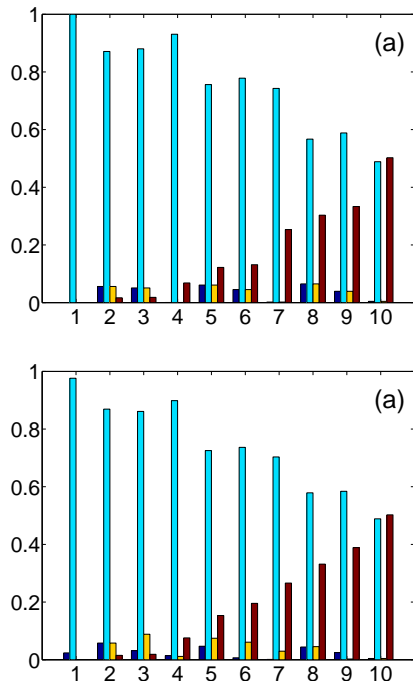


Figure 6: (Color online). A single particle’s probability distributions as a function of time for the first nine steps for a particle in a double well potential. The two potential wells are at  $|01\rangle$  (lattice point 2) and  $|11\rangle$  (lattice point 4). (a) The theoretical predictions; (b) The liquid NMR experimental results. The four bars at each step indicates the particle’s probability on the state  $|00\rangle$  (blue),  $|01\rangle$  (green),  $|10\rangle$  (yellow),  $|11\rangle$  (red), from left to right. The initial state is prepared in  $|01\rangle$ . As is illustrated in (a) and (b), the particle tunnels from  $|01\rangle$  to  $|11\rangle$ . Our experiments agrees quite well with theoretical results depicted, clearly manifesting the tunneling phenomenon.

parameters except for the removal of the potential operator  $P$  in the circuit, and its corresponding RF pulse sequences were also performed from one to nine times. The final state reconstructed by full QST is shown in Fig. 5 with a fidelity 96.82% according to Eq. (17). The results of these nine experiments, together with the theoretical calculations, are plotted in Fig. 7 to illustrate the evolution of a free particle. It is not surprising to find that the probability distributed more evenly on all the four lattice points, considering the particle is free.

Our experiments have simulated the fundamental quantum phenomenon of tunneling and reflected an evident difference between the two situations with and without the double well potential. It should be emphasized here that although the real evolution of the particle takes place in a continuous space with infinite dimension, the quantum computer via only a few qubits with limited dimension (in our case four dimension) is already capable of undertaking some basic yet fundamental simulation tasks such as the quantum tunneling. The result has re-

vealed the amazing power hidden under the qubits and

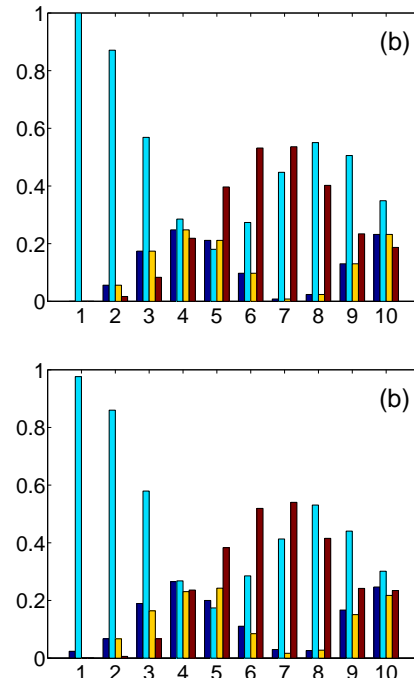


Figure 7: (Color online). The free particle’s probability distributions as a function of time for the first nine steps. (a) The theoretical predictions; (b) The liquid NMR experimental results. The four bars at each step indicates the particle’s probability on the state  $|00\rangle$  (blue),  $|01\rangle$  (green),  $|10\rangle$  (yellow),  $|11\rangle$  (red), from left to right. The initial state is prepared to be  $|01\rangle$ . As is illustrated in (a) and (b), the particle’s probability becomes more evenly distributed among all the four states. Our experiments agrees quite well with theoretical results depicted.

the promising future of quantum computation.

In summary, we accomplished a small scale demonstration of the quantum tunneling process on the 2-qubit NMR system based on the digital quantum simulation method. As far as our knowledge concerns this is the first demonstration work on quantum tunneling simulation via NMR quantum information processor. The experimental results and the theoretical predictions are in good agreement. The overlaps of final states after nine steps of evolution (with and without the double well potential) between the experimental results and the theoretical predictions are about 95% which manifests the high quality of the experimental results.

This work was supported by the National Natural Science Foundation of China (Grant No. 10874 098), the National Basic Research Program of China (2009CB929402, 2011CB9216002), and the Specialized Research Fund for the Doctoral Program of Education Ministry of China (2006 0003048).

- 
- [1] Richard P. Feynman, International Journal of theoretical Physics 21, 467(1982).
- [2] E. Gerjuoy, Am. J. Phys. 73, 521-540 (2005).
- [3] L. K. Grover, Rhys. Rev. Lett. 79, 325(1997).
- [4] C.H. Tseng, S. Somaroo, Y. Sharf, E. Knill, R. Laflamme, T.F. Havel and D.G. Cory, Phys. Rev. A, 61:012302, 1999.
- [5] C. Negrevergne, R. Somma, G. Ortiz, E. Knill and R. Laflamme, Phys. Rev. A, 71:032344, 2005.
- [6] X.H. Peng, J.F. Zhang, J.F. Du and D. Suter, Phys. Rev. Lett., 103:140501, 2009.
- [7] X.H. Peng, J.F. Du and D. Suter, Phys. Rev. A, 71:012307, 2005.
- [8] E.E. Edwards, S. Korenblit, K. Kim, R. Islam, M.- S. Chang, J.K. Freericks, G.-D. Lin, L.-M. Duan and C. Monroe, Phys. Rev. B, 82:060412, 2010.
- [9] B.P. Lanyon, J.D. Whitfield, G.G. Gillett, M.E. Goggin, M.P. Almeida, I. Kassal, J.D. Biamonte, M. Mohseni, B.J. Powell, M. Barbieri, A. Aspuru-Guzik and A.G. White, Nature Chemistry, 2:106111, 2010.
- [10] J.F. Du, N.Y. Xu, X.H. Peng, P.F. Wang, S.F. Wu and D.W. Lu, Phys. Rev. Lett., 104:030502, 2010.
- [11] C. Zalka, Proc. R. Soc. Lond. A, 454:3135C322, 1998.
- [12] G. Benenti and G. Strini, Am. J. Phys., 76:657-662, 2008.
- [13] I. Kassal, J.D. Whitfield, A. Perdomo-Ortiz, M.-H. Yung and A. Aspuru-Guzik, Annu. Rev. Phys. Chem., 62:185-207, 2011.
- [14] I. Kassal, S.P. Jordan, P.J. Love, M. Mohseni and A. Aspuru-Guzik, Proc. Nat. Acad. Sci. USA, 105:18681-18686, 2008.
- [15] B. D. Josephson, Phys. Lett. 1, 251 (1962).
- [16] Leo Esaki and Yuriko Miyahara, Solid-State Electronics 1, 13(1960).
- [17] G. Binnig and H. Rohrer, IBM Journal of Reserch and Development 44, 279-293(2000)
- [18] Andrew T. Sornborger, arXiv:1202.1536v1 (2012). In our work, we exchanged the  $c_0$  in  $Z_0$  with  $c_1$  in  $Z_1$ .
- [19] D. Coppersmith, IBM Research Report, RC19642, 1994.
- [20] David G. Cory, Mark D. Price and Timothy F. Havel, Physica D: Nonlinear Phenomena 120, 82 (1998).
- [21] Jae-Seung Lee, Phys. Lett. A 305, 349(2002).
- [22] G L Long, H Y Yan and Y Sun, J. Opt. B: Quantum Semiclass. Opt. 3, 376 (2001).